Progress In Electromagnetics Research, PIER 40, 71–90, 2003

LENGTH REDUCTION OF EVANESCENT-MODE RIDGE WAVEGUIDE BANDPASS FILTERS

T. Shen

Advanced Development Group
Hughes Network Systems
Germantown, MD 20876, USA

K. A. Zaki

Department of Electrical and Computer Engineering
University of Maryland
College Park, MD 20742, USA

Abstract—Length reduction of evanescent-mode ridge waveguide bandpass filters is investigated extensively. Based on the conventional filter configuration, two new filter configurations are proposed: one is the generalized filter, and the other is the folded filter. In the generalized filter configuration, the cross sections of the evanescent waveguide and the ridge waveguide are not necessarily the same. It is found that the filter length can be reduced by enlarging the evanescent waveguide height. In the folded filter configuration, the filter is folded back at the middle coupling section. The folded junction is ridged to provide the required coupling between the two ridge waveguide resonators it connects. A design example demonstrates the feasibility of this filter configuration.

1. INTRODUCTION

Compared to rectangular waveguides, ridge waveguides [1, 2] have the advantages of wide fundamental-mode operation bandwidth, low cutoff frequency, and low wave impedance. Fundamental-mode operation bandwidth of five to one or more is easily obtainable with ridge waveguides. The low cutoff frequency yields a small cross section and hence a compact size of ridge waveguide components. The low wave impedance permits an easy transition to planar transmission lines such as strip lines or microstrip lines. In addition, there is a great deal of flexibility in ridge configuration according to different electrical and mechanical requirements [3]. Some common ridge configurations include: single or double ridge, triple ridge, and single or double antipodal ridge. Because of these advantages, ridge waveguides have found extensive applications in microwave active and passive components, including filters.

Evanescent-mode ridge waveguide filters have drawn considerable attention in the recent past because of their relatively wide spurious-free out-of-band response, compact size, and reduced weight. In [4–6] evanescent-mode ridge waveguide lowpass and bandpass filters are presented, where various ridge configurations are used and wide spurious-free out-of-band response is achieved. Recently, evanescent-mode ridge waveguide bandpass filters are implemented successfully in LTCC (Low Temperature Cofired Ceramics) [7, 8].

As mentioned above, compared to rectangular waveguides, ridge waveguides have a lower fundamental-mode cutoff frequency. Hence, ridge waveguide filters have a smaller cross section than rectangular waveguide filters. However, the lengths of the two types of filters are comparable with each other. Many applications require ridge waveguide filters with substantially reduced length. In [6], serrations are introduced in the ridge waveguide to reduce the resonator length and suppress the spurious response. In this paper, length reduction of evanescent-mode ridge waveguide bandpass filters is investigated extensively. For this purpose, based on the conventional filter configuration, two new filter configurations are proposed, as shown

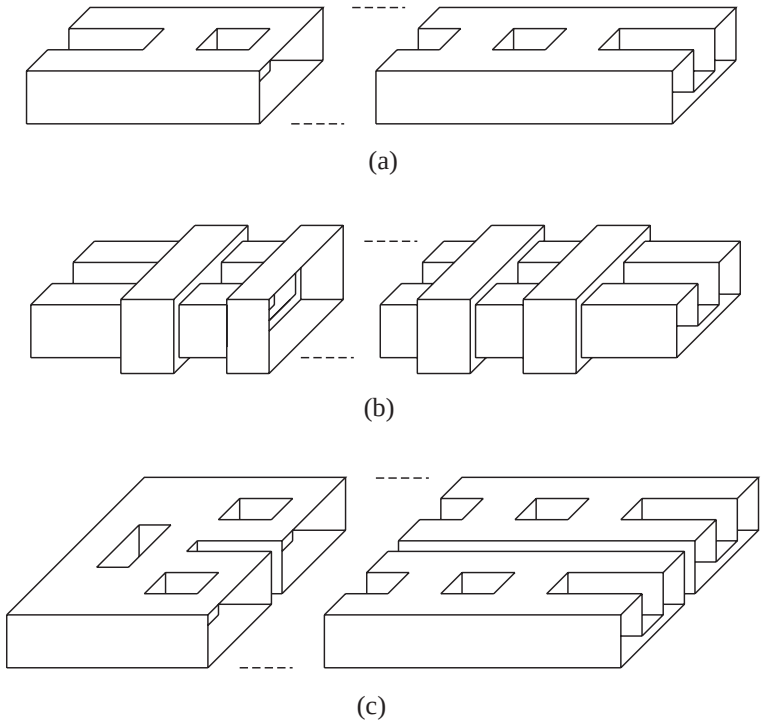

Figure 1. Evanescent-mode ridge waveguide bandpass filters. (a) Conventional configuration. (b) Generalized configuration. (c) Folded configuration.

in Fig. 1.

In the conventional filter configuration shown in Fig. 1(a), the evanescent waveguide (used as the impedance inverter) has the same cross section as the ridge waveguide (used as the resonator). In the generalized filter configuration shown in Fig. 1(b), the cross sections of the evanescent waveguide and the ridge waveguide are not necessarily the same. It is found that the filter length can be reduced by enlarging the evanescent waveguide height. In addition, the effect of the fundamental-mode cutoff frequency and the ridge gap height of the ridge waveguide on the filter length is investigated. In the folded filter configuration shown in Fig. 1(c), the filter is folded back at the middle coupling section. The folded junction is ridged to provide the required coupling between the two ridge waveguide resonators it connects.

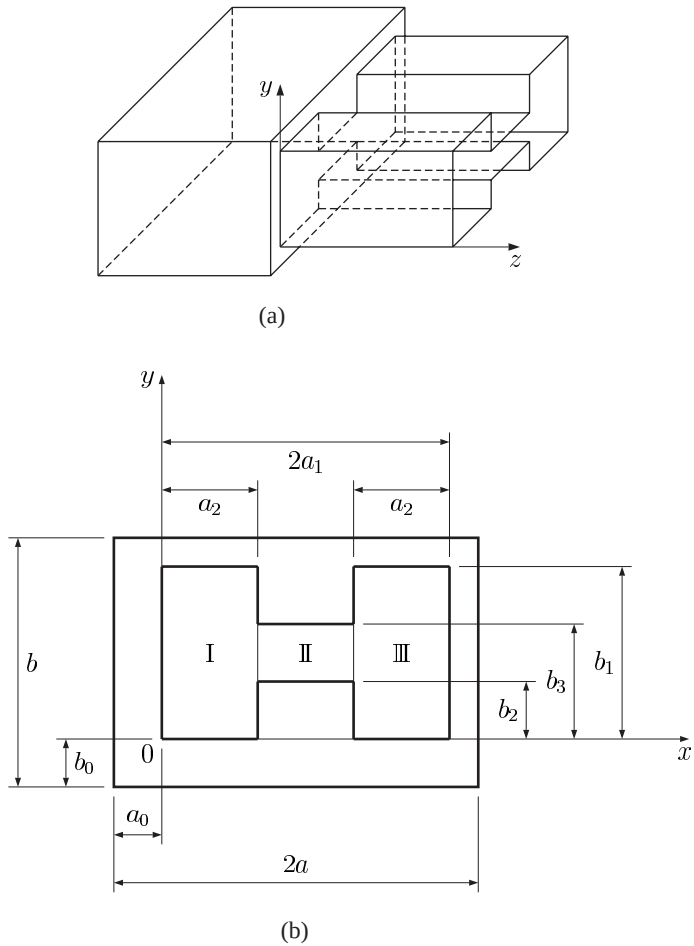

Figure 2. Empty-to-ridge waveguide discontinuity. (a) Configuration. (b) Discontinuity plane.

2. GENERALIZED FILTER

2.1. Modeling, Optimization, and Synthesis

For full-wave modeling, the generalized filter structure shown in Fig. 1(b) is decomposed into the cascade connection of the empty-to-ridge waveguide discontinuity shown in Fig. 2. The generalized scattering matrix of the discontinuity is obtained using mode matching method [9]. Fig. 3 shows the comparison between mode-matching results and HFSS results of scattering parameters for a structure

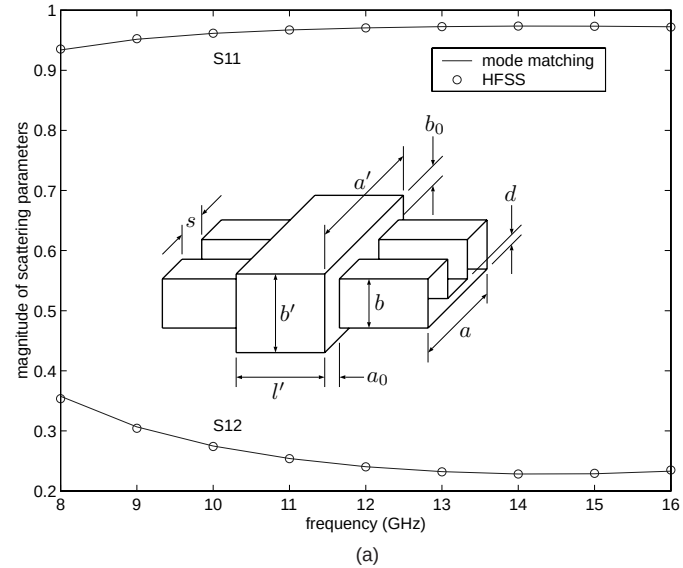

(a)

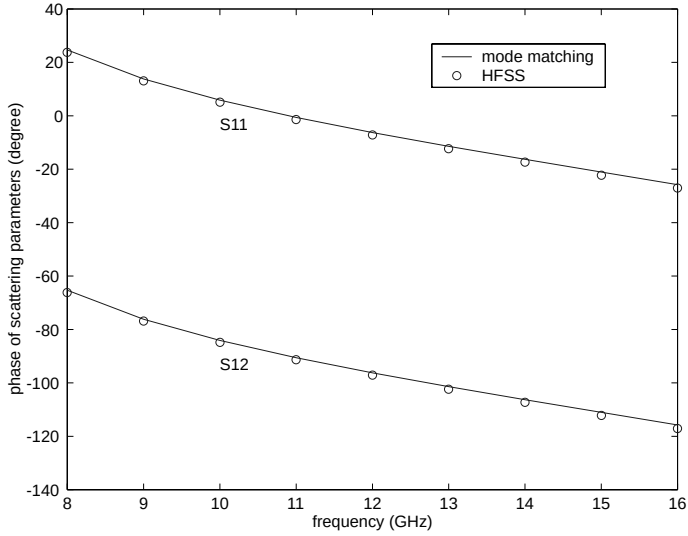

(b)

Figure 3. Scattering parameters of a structure composed of two identical back-to-back cascaded empty-to-ridge waveguide discontinuities. (a) Magnitude. (b) Phase. The structure dimensions in mils are: $a = 180, b = 80, s = 36, d = 12, a' = 210, b' = 80, a_0 = 30, b_0 = 0$, and $l' = 100$. The structure is dielectric-filled ($\epsilon_r = 6$).

composed of two identical back-to-back cascaded empty-to-ridge waveguide discontinuities. A good agreement is observed. Once the generalized scattering matrix of the empty-to-ridge waveguide discontinuity is available, the overall generalized scattering matrix of the filter can be obtained using cascading procedure. Note that the conventional filter structure shown in Fig. 1(a) can be regarded as a specific case of the generalized filter structure.

For optimization design, according to the design specification, an error function to be minimized is constructed with the lengths of both ridge waveguide and evanescent waveguide as optimization variables. The initial values of these optimization variables are obtained from synthesis, which is described briefly as below.

In the evanescent-mode ridge waveguide bandpass filter, the impedance inverter is realized using the evanescent waveguide operating below its fundamental-mode cutoff frequency, while the series resonator between the impedance inverters is realized using the ridge waveguide. In the practical design, the empty-to-ridge waveguide discontinuity effect should be taken into account. The impedance inverter is composed of two identical such discontinuities cascaded together through a section of evanescent waveguide. The value of the impedance inverter (which physically represents the coupling between the two resonators it connects) can be obtained from its scattering parameters [10]. The cross section and the length of the evanescent waveguide can be adjusted to achieve the synthesized value of the impedance inverter. Once the impedance inverter is determined, the ridge waveguide length (180 degrees nominally) is shortened to subtract the empty-to-ridge waveguide discontinuity effect.

In the conventional filter configuration, since the evanescent waveguide has the same cross section as the ridge waveguide, the synthesized value of the impedance inverter is achieved by adjusting the evanescent waveguide length only. In the generalized filter configuration, however, the cross sections of the evanescent waveguide and the ridge waveguide are not necessarily the same. This provides two more degrees of freedom in achieving the synthesized value of the impedance inverter. By choosing an optimal cross section of the evanescent waveguide, the filter length may be minimized.

2.2. Cross-Section Configuration of Ridge Waveguide

The cross-section configuration of the ridge waveguide is usually determined according to its fundamental-mode operation bandwidth, power handling capacity, and attenuation property. Fig. 4 shows the normalized fundamental-mode cutoff wavelength λ_c/a of the ridge waveguide as a function of d/b ratio, with b/a and s/a ratios fixed at

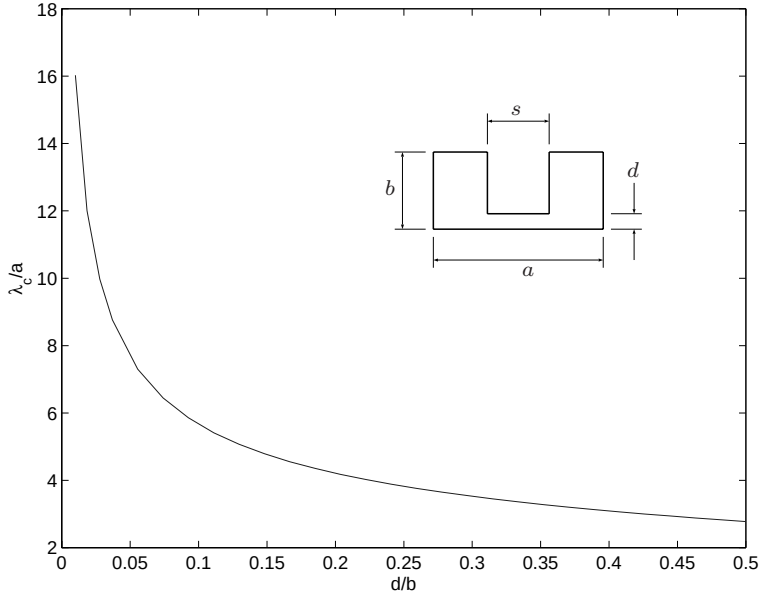

Figure 4. Normalized fundamental-mode cutoff wavelength λ_c/a of the ridge waveguide versus d/b ratio. $b/a = s/a = 0.45$.

typical 0.45. The standard b/a ratio is 0.45. For a given d/b ratio, the maximum fundamental-mode operation bandwidth is achieved when the s/a ratio is around 0.45 [2, 11]. The normalized cutoff wavelength curve in Fig. 4 remains nearly the same when the b/a and s/a ratios are in the range of 0.4 to 0.5. From Fig. 4, it is seen that the normalized cutoff wavelength λ_c/a increases with the d/b ratio decreased. Hence, a small ridge gap height yields a compact cross section of the ridge waveguide. However, decreasing the ridge gap height too much will increase the loss and reduce the power handling capacity of ridge waveguide components.

Given a fundamental-mode cutoff wavelength (or frequency) and a d/b ratio, the cross-section dimensions of the ridge waveguide can be determined according to Fig. 4. It will be seen later that the fundamental-mode cutoff frequency and the ridge gap height of the ridge waveguide have a considerable effect on the filter length. In addition, the filter spurious response can be improved considerably by decreasing the ridge gap height.

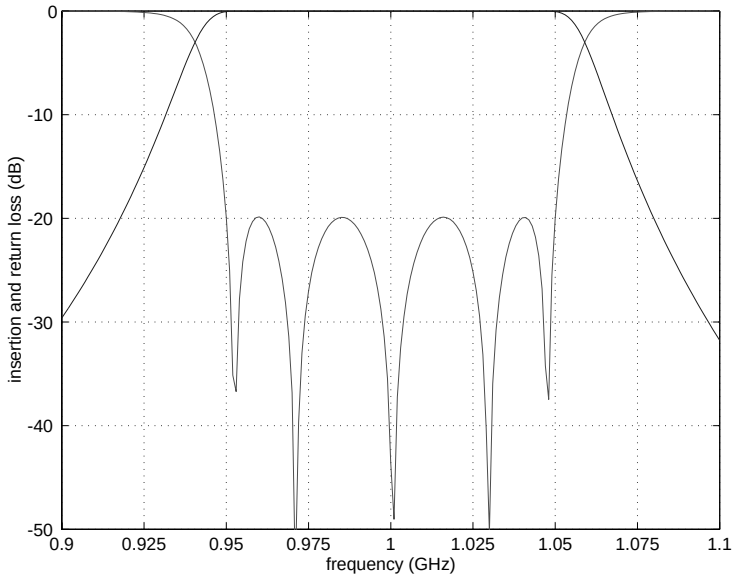

Figure 5. Computed response of the five-section 1-GHz filter.

2.3. Length Reduction: Table 1

Using the generalized filter configuration, a five-section 1-GHz filter of bandwidth of 0.1 GHz and passband return loss of 20 dB is designed. For the potential LTCC implementations, the filter is assumed to be filled with the dielectric material of relative dielectric constant $\epsilon_r = 6$. The typical computed response of the filter is shown in Fig. 5.

Table 1 gives one set of dimensions of the filter designed using different cross-section configurations of the ridge waveguide and the evanescent waveguide. The dimension notations used in Table 1 (and Table 2 which will be given later) are illustrated in Fig. 6. Three ridge waveguides (denoted as RG1, RG2, and RG3) are used. The main difference of the three ridge waveguides is the fundamental-mode cutoff frequency f_c. The first one (RG1) has the highest f_c (0.838 GHz), the third one (RG3) the lowest (0.723 GHz), and the second one (RG2) in between (0.822 GHz). For each ridge waveguide, three evanescent waveguides of different heights (and the same width as the ridge waveguide) are used. The first row for each ridge waveguide gives the length dimensions of the filter using the evanescent waveguide of the same height as the ridge waveguide ($b' = b$).

From Table 1, it is found that enlarging the evanescent waveguide height can reduce the lengths of both ridge waveguide and evanescent

Table 1. Dimensions (given in inches) of the five-section 1-GHz filter. Refer to Fig. 6 for dimension notations. RG1, RG2, and RG3 denote the three ridge waveguides used. R denotes the length reduction in percentage. The evanescent waveguide has the same width as the ridge waveguide ($a' = a$). The aspect ratios b/a, s/a, and d/b of the ridge waveguide are fixed at 0.45, 0.45, and 0.15, respectively.

b'	l'			l			L	R
	1 (6)	2 (5)	3 (4)	1 (5)	2 (4)	3		
RG1: $a = 1.2, f_c = 0.838\,\text{GHz}$								
b	0.2514	0.5920	0.7273	1.1557	0.9381	0.9086	8.2378	
0.75	0.1814	0.5081	0.6624	1.1049	0.8134	0.7730	7.3188	11%
1.00	0.1534	0.4321	0.5814	1.0450	0.7442	0.6981	6.6104	20%
RG2: $a = 1.23, f_c = 0.822\,\text{GHz}$								
b	0.2702	0.6505	0.7962	1.0219	0.8109	0.7857	7.8852	
0.85	0.1840	0.5339	0.7050	0.9483	0.6624	0.6264	6.6934	15%
1.10	0.1565	0.4575	0.6175	0.9216	0.6361	0.5968	6.1752	22%
RG3: $a = 1.4, f_c = 0.723\,\text{GHz}$								
b	0.3406	0.9530	1.1591	0.5243	0.3482	0.3365	6.9868	
0.95	0.2242	0.8033	1.0561	0.5093	0.2855	0.2702	6.0270	14%
1.25	0.1822	0.6713	0.9250	0.4999	0.2759	0.2574	5.3658	23%

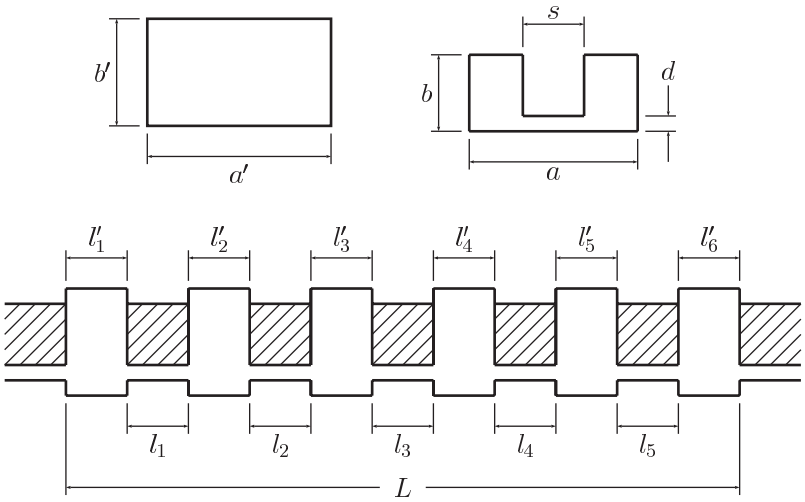

Figure 6. Dimension notations used in Tables 1 and 2 for the five-section 1-GHz filter.

Table 2. Dimensions (given in inches) of the five-section 1-GHz filter. Refer to Fig. 6 for dimension notations. RG1, RG2, and RG3 denote the three ridge waveguides used. R denotes the length reduction in percentage. The evanescent waveguide has the same width as the ridge waveguide ($a' = a$). The aspect ratios b/a and s/a of the ridge waveguide are fixed at 0.45. Note that the three ridge waveguides (RG1, RG2, and RG3) have the same fundamental mode cutoff frequency $f_c \approx 0.76\,\text{GHz}$.

b'	l'			l			L	R
	1 (6)	2 (5)	3 (4)	1 (5)	2 (4)	3		
RG1: $a = 1.34, d = 0.15b = 0.0905\,\text{GHz}$								
b	0.3211	0.8543	1.0399	0.6483	0.4623	0.4477	7.0995	
0.90	0.2149	0.7170	0.9426	0.6209	0.3798	0.3601	6.1106	14%
1.00	0.1820	0.6214	0.8452	0.6010	0.3608	0.3385	5.5592	22%
RG2: $a = 1.02, d = 0.08b = 0.0367\,\text{GHz}$								
b	0.1946	0.5643	0.7030	0.6912	0.4954	0.4805	5.7775	
0.85	0.1343	0.4705	0.6300	0.6550	0.4183	0.3992	5.0155	13%
1.10	0.1160	0.4161	0.5711	0.6253	0.3886	0.3683	4.6024	20%
RG3: $a = 0.66, d = 0.03b = 0.0089\,\text{GHz}$								
b	0.0907	0.3127	0.4086	0.6491	0.4321	0.4169	4.2033	
0.45	0.0655	0.2664	0.3735	0.5906	0.3480	0.3305	3.6186	14%
1.25	0.0568	0.2391	0.3435	0.5624	0.3187	0.3006	3.3416	20%

waveguide, and hence the total length of the filter. More than 20% length reduction (denoted as R) for all three ridge waveguides can be achieved.

From Table 1, it is also found that the fundamental-mode cutoff frequency of the ridge waveguide has a considerable effect on the filter length. The filter length can be reduced using the ridge waveguide of lower cutoff frequency. For instance, considering the $b' = b$ case, the filter using the ridge waveguide of $f_c = 0.838\,\text{GHz}$ has a length of 8.2378 inches, while the filter using the ridge waveguide of $f_c = 0.723\,\text{GHz}$ has a length of 6.9868 inches. This can be explained by the relation between the guided wavelength λ_g and the fundamental-mode cutoff frequency f_c of a waveguide

$$\lambda_g = \frac{\lambda}{\sqrt{1 - \left(\frac{f_c}{f}\right)^2}}$$

where λ and f are the operating wavelength and frequency, respectively. From the above relation, it is seen that a low cutoff frequency f_c results in a short guided wavelength λ_g, and hence a short waveguide resonator length ($\lambda_g/2$ nominally). As mentioned above, ridge waveguides have wide fundamental-mode operation bandwidth, which provides a great deal of flexibility in the choice of the cutoff frequency according to different applications.

Another interesting observation from Table 1 is that the fundamental-mode cut off frequency of the ridge waveguide determines the length ratio of the ridge waveguide to the evanescent waveguide. When the cutoff frequency is close to the filter band, the ridge waveguide length is larger than the evanescent waveguide length. With the cutoff frequency moving away from the filter band, the ridge waveguide length decreases, and the evanescent waveguide length increases. Finally, when the cutoff frequency is (relatively) far from the filter band, the evanescent waveguide length is much larger than the ridge waveguide length. Actually the concept of evanescent-mode waveguide bandpass filters [12, 13] refers to this latter case, in which compared with the evanescent waveguide, the ridge waveguide is so small that it can be viewed as a capacitive screw. When the ridge waveguide length is much larger than the evanescent waveguide length, the filter operates more like a direct-coupled (ridge waveguide) cavity filter with the evanescent waveguide as the coupling element. At some intermediate stage where the ridge waveguide length is approximately the same as the ridge width s, the filter can be regarded as a combline filter with the ridge as the TEM resonator line.

2.4. Length Reduction: Table 2

Table 2 gives another set of dimensions of the filter. Like Table 1, three ridge waveguides (RG1, RG2, and RG3) are used, and for each ridge waveguide, three evanescent waveguides of different heights are used. The main difference of the three ridge waveguides is the d/b ratio (ridge gap height). The first one (RG1) has the highest d/b ratio (0.15), the third one (RG3) the lowest (0.03), and the second one (RG2) in between (0.08). For the sake of comparison, the three ridge waveguides have the same fundamental-mode cutoff frequency $f_c \approx 0.76\,\text{GHz}$. Again, it is found that enlarging the evanescent waveguide height can reduce the lengths of both ridge waveguide and evanescent waveguide, and hence the total length of the filter.

From Table 2, it is also found that the ridge gap height (d/b ratio) has a considerable effect on the filter length. The filter length can be reduced using the ridge waveguide of smaller ridge gap height. For instance, considering the $b' = b$ case, the filter using the ridge

waveguide of $d = 0.15b = 0.0905$ inch has a length of 7.0995 inches, while the filter using the ridge waveguide of $d = 0.03b = 0.0089$ inch has a length of 4.2033 inches. Careful inspection of Table 2 shows that the ridge gap height has much more effect on the evanescent waveguide length than the ridge waveguide length. With the ridge gap height (d/b ratio) decreased, the evanescent waveguide length decreases considerably while the ridge waveguide length remains in the same order. Most of the length reduction of the filter results from the length reduction of the evanescent waveguide. This is due to the fact that the three ridge waveguides in Table 2 have the same fundamental-mode cutoff frequency. Ideally, without considering the subtraction effect of the ridge-to-rectangular waveguide discontinuity, the ridge waveguide length ($\lambda_g/2$ nominally) should always be the same for different ridge waveguides of the same cutoff frequency.

2.5. Further Discussion

From Tables 1 and 2, it can be found that more than 50% length reduction can be achieved by configuring the ridge waveguide properly and enlarging the evanescent waveguide height (the first filter in Table 1 has a length of 8.2378 inches, while the last filter in Table 2 has a length of 3.3416 inches).

It is found that enlarging the evanescent waveguide width has little effect on the length reduction or even increases the filter length in some cases. A reasonable explanation is that the evanescent waveguide becomes less "evanescent" with an enlarged width. It is also found that using the evanescent waveguide of smaller width than the ridge waveguide could reduce the evanescent waveguide length a little. However the ridge waveguide length is increased, and the total length of the filter is not reduced.

Enlarging the evanescent waveguide height to reduce the filter length is virtually the same as decreasing the ridge gap height to reduce the filter length. Both disturb the field distribution and hence the property of the empty-to-ridge waveguide discontinuity in such a way that the filter length is reduced. This can also explain why varying the evanescent waveguide width has little effect on the filter length. The field distribution at the discontinuity is hardly disturbed by varying the evanescent waveguide width, since in the ridge waveguide, the fundamental-mode field is concentrated under the ridge gap, as shown in Fig. 7.

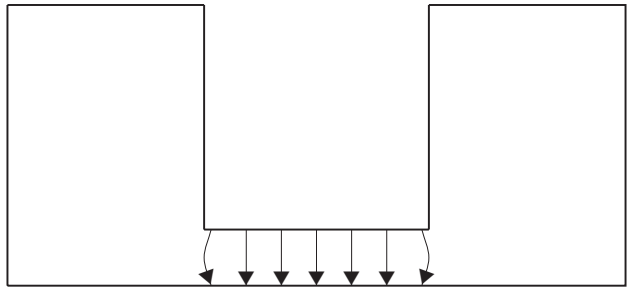

Figure 7. (Electric) field distribution of the ridge waveguide.

2.6. Spurious Response Consideration

Figs. 8(a) and (b) show the spurious responses of the filters using the ridge waveguides in Table 1 of $f_c = 0.822\,\text{GHz}$ and $f_c = 0.723\,\text{GHz}$, respectively. It is seen that enlarging the evanescent waveguide height has no definite effect on the filter spurious response.

Fig. 9 shows the spurious responses of the filters using the ridge waveguide in Table 2 of $d = 0.03b = 0.0089$ inch. Compared to the spurious responses shown in Fig. 8 (where $d = 0.15b$), it is seen that decreasing the ridge gap height can considerably improve the filter spurious response. As shown in Fig. 9(a) where the evanescent waveguide has the same height as the ridge waveguide, spurious-free response of more than sixth harmonics is achieved (except two 80-dB spikes at 3.7 GHz and 5.3 GHz). It is seen from Fig. 9(b) that although enlarging the evanescent waveguide height reduces the range of spurious-free response by one harmonic, the two spikes in Fig. 9(a) are eliminated.

Although the filter length can be reduced and the spurious response can be improved by decreasing the ridge gap height, in practice, however, since the ridge gap height cannot be too small due to Q (quality factor) and power handling requirement and fabrication difficulty, the filter length reduction and the spurious response improvement are limited.

3. FOLDED FILTER

3.1. Modeling and Synthesis

For the sake of modeling convenience, the folded filter structure shown in Fig. 1(c) is assumed to be symmetric with respect to the folded junction. Therefore, the (dominant-mode) scattering parameters

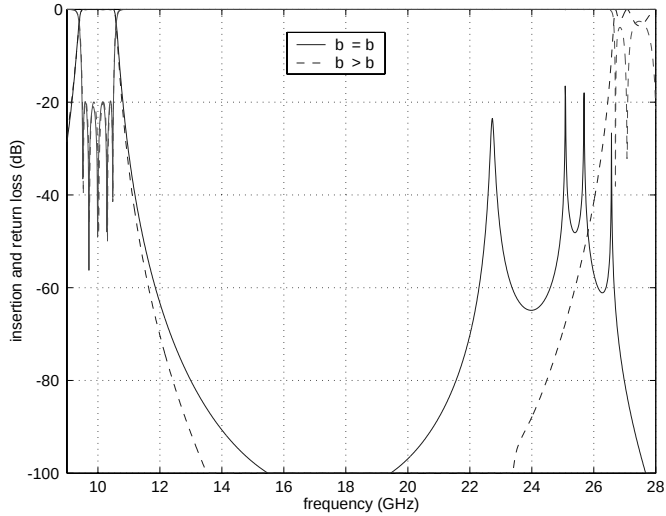

(a)

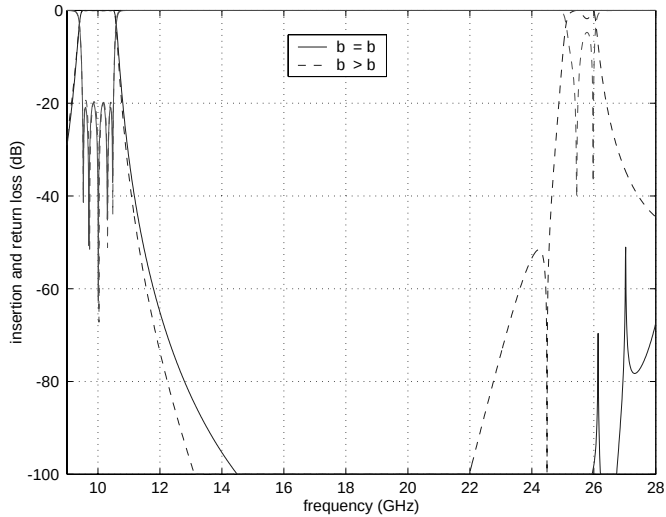

(b)

Figure 8. Spurious responses of two filters. (a) The filter dimensions are given in Table 1 for the ridge waveguide of $f_c = 0.822\,\text{GHz}$. The solid line is for $b' = b = 0.5535$ inch. The dashed line is for $b' = 1.1$ inches. (b) The filter dimensions are given in Table 1 for the ridge waveguide of $f_c = 0.723\,\text{GHz}$. The solid line is for $b' = b = 0.63$ inch. The dashed line is for $b' = 1.25$ inch.

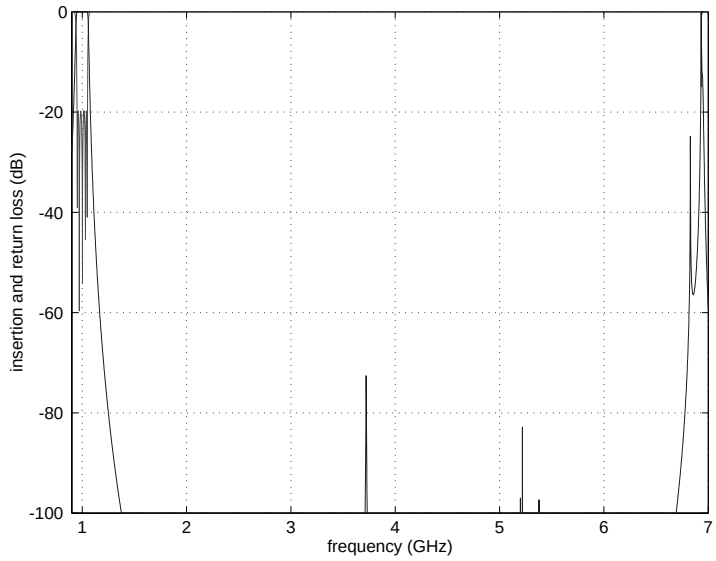

(a)

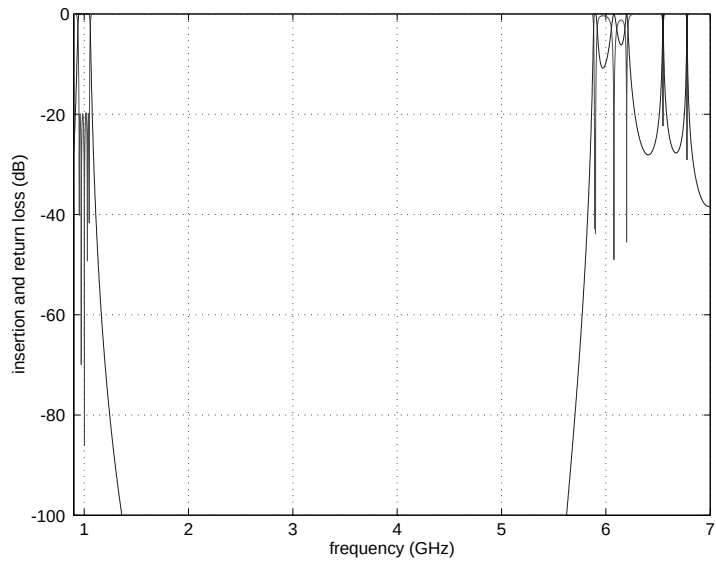

(b)

Figure 9. Spurious responses of two filters. The filter dimensions are given in Table 2 for the ridge waveguide of $d = 0.03b = 0.0089$ inch. (a) $b' = b = 0.297$ inch. (b) $b' = 0.45$ inch.

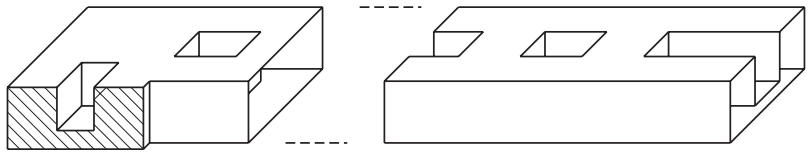

Figure 10. Half structure of the folded filter configuration shown in Fig. 1(c). The shaded area is either PEC of PMC boundary condition.

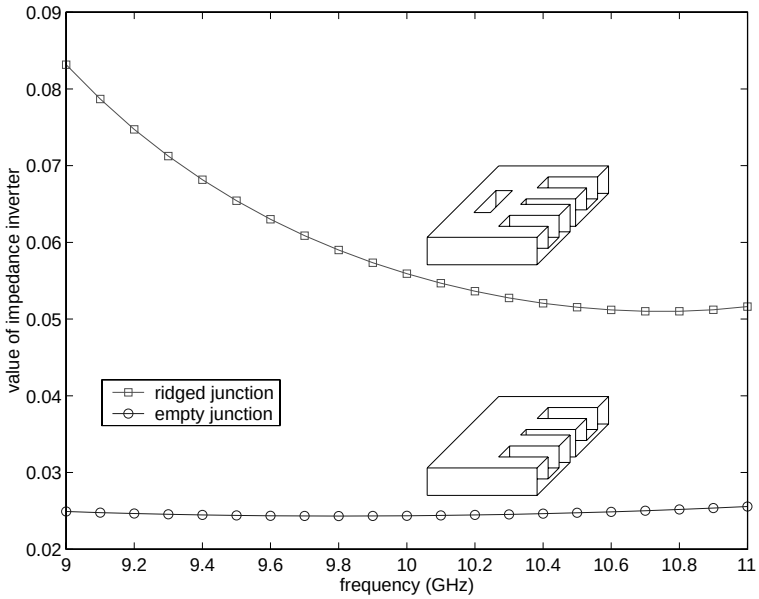

Figure 11. Comparison of values of impedance inverter for a folded junction with and without being ridged. The junction dimensions are given in Fig. 12(a).

of the filter can be obtained by modeling the half structure twice with PEC (Perfect Electric Conductor) and PMC (Perfect Magnetic Conductor) boundary conditions placed at the (shaded) symmetry plane, as shown in Fig. 10. The half structure is decomposed into the cascade connection of empty-to-ridge waveguide discontinuities. The generalized scattering matrix of the discontinuity is obtained using mode matching method, and then the filter response is obtained using cascading procedure, as described in the last section. However, note that since the discontinuity encountered in this filter configuration is not symmetric with respect to the ridge waveguide cross-section

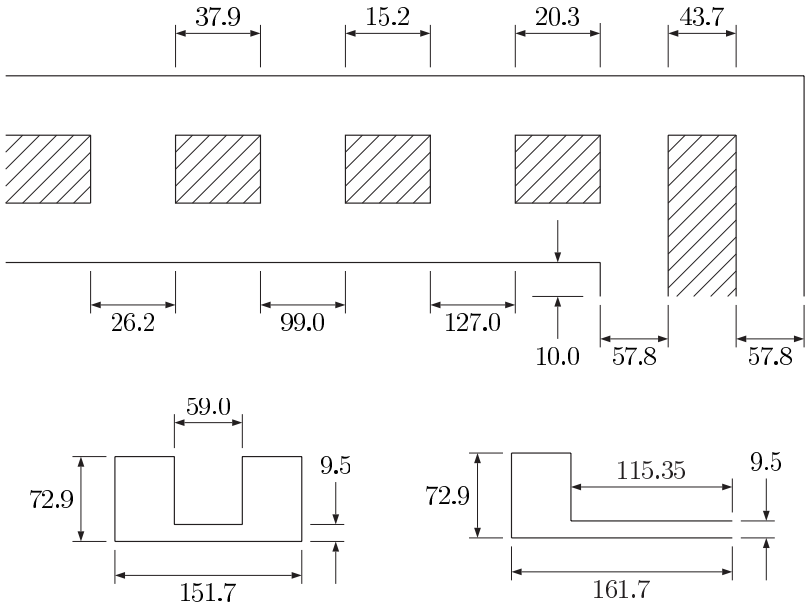

(a)

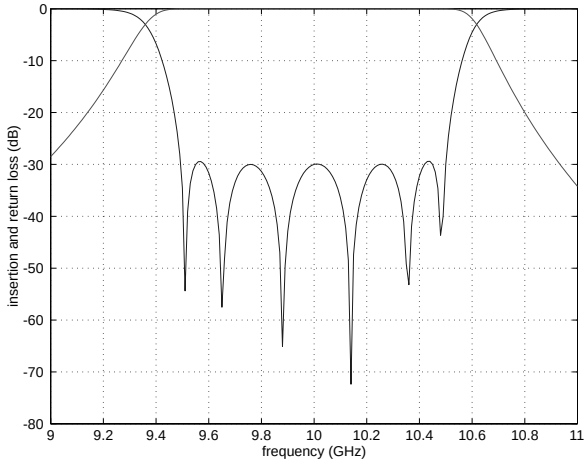

(b)

Figure 12. (a) Dimensions (given in mils) of half the six-section 10-GHz filter. Only half dimensions are shown here since the filter is symmetric with the folded junction. The structure is dielectric-filled ($\epsilon = 5.76$). (b) Computed response of the six-section 10-GHz filter.

mid-plane, both PMC and PEC ridge waveguide eigenmodes should be included in the discontinuity computation. On the contrary, in the conventional and generalized filter configurations, since the filter structure is symmetric with respect to the ridge waveguide cross-section mid-plane, only PMC ridge (and empty) waveguide eigenmodes are included in the computation of the empty-to-ridge waveguide discontinuity and the following cascading procedure.

In the folded filter configuration, the impedance inverter is realized using either the evanescent waveguide (*straight* inverter) or the folded junction (*folded* inverter). For the *straight* impedance inverter, the evanescent waveguide length can be adjusted to achieve the synthesized coupling value. For the *folded* impedance inverter, it is found that the empty folded junction cannot provide the required coupling value between the two ridge waveguide resonators it connects. Therefore. the folded junction is ridged to increase the coupling. The dimensions of the ridge and the junction itself can be adjusted to achieve the synthesized coupling value. As shown in Fig. 11, the coupling value of a folded junction increases from 0.025 (without ridge) to 0.055 (with ridge) at 10 GHz.

3.2. Design Example

Using the folded filter configuration, a six-section 10-GHz filter of bandwidth of 1 GHz and passband return loss of 30 dB is designed. The filter is assumed to be filled with the dielectric material of relative dielectric constant $\epsilon_r = 5.76$. The optimized filter dimensions are given in Fig. 12(a), and the corresponding filter response is shown in Fig. 12(b). The design example demonstrates the feasibility of the folded filter configuration.

4. SUMMARY

Length reduction of evanescent-mode ridge waveguide bandpass filters is investigated extensively. Based on the conventional filter configuration, two new filter configurations are proposed: one is the generalized filter, and the other is the folded filter. In the generalized filter configuration, the cross sections of the evanescent waveguide and the ridge waveguide are not necessarily the same. It is found that the filter length can be reduced by enlarging the evanescent waveguide height. It is also found that the filter length can be reduced using the ridge waveguide of lower fundamental-mode cutoff frequency and smaller ridge gap height. More than 50% filter length reduction can be achieved by configuring the ridge waveguide properly and enlarging the

evanescent waveguide height. In addition, the filter spurious response can be improved considerably by decreasing the ridge gap height. In the folded filter configuration, the filter is folded back at the middle coupling section. The folded junction is ridged to provide the required coupling between the two ridge waveguide resonators it connects. A design example demonstrates the feasibility of this filter configuration.

REFERENCES

1. Cohn, S. B., "Properties of ridge waveguide," *Proc. IRE*, Vol. 35, 783–788, Aug. 1947.
2. Hopfer, S., "The design of ridged waveguides," *IRE Trans. Microwave Theory Tech.*, Vol. MTT-5, 20–29, Oct. 1955.
3. Saad, A. M. K., "A unified ridge structure for evanescent-mode wideband harmonic filters: analysis and applications," *17th European Microwave Conf. Proc.*, 157–162, Rome, Italy, 1987.
4. Saad, A. M. K., "Novel lowpass harmonic filters for satellite application," *IEEE MTT-S Int. Microwave Symp. Dig.*, 292–294, San Francisco, CA, May 1984.
5. Saad, A. M. K., J. D. Miller, A. Mitha, and R. Brown, "Analysis of antipodal ridge waveguide structure and application on extremely wide stopband lowpass filter," *IEEE MTT-S Int. Microwave Symp. Dig.*, 361–363, Baltimore, MD, June 1986.
6. Saad, A. M. K., A. Mitha, and R. Brown, "Evanescent mode-serrated ridge waveguide bandpass harmonic filters," *16th European Microwave Conf. Proc.*, 287–291 Dublin, Ireland, 1986.
7. Gipprich, J., D. Stevens, M. Hageman, A. Piloto, K. A. Zaki, and Y. Rong, "Embedded waveguide filters for microwave and wireless applications using cofired ceramic technologies," *Proc. Int. Symp. Microelectron.*, 23, San Diego, CA, Nov. 1998.
8. Rong, Y., K. A. Zaki, M. Hageman, D. Stevens, and J. Gipprich, "Low-temperature cofired ceramic (LTCC) ridge waveguide bandpass chip filters," *IEEE Trans. Microwave Theory Tech.*, Vol. 47, 2317–2324, Dec. 1999.
9. Wang, C. and K. A. Zaki, "Full-wave modeling of generalized double ridge waveguide T-junctions," *IEEE Trans. Microwave Theory Tech.*, Vol. 44, 2536–2542, Dec. 1996.
10. Yao, H.-W., A. E. Abdelmonem, J.-F. Liang, X.-P. Liang, K. A. Zaki, and A. Martin, "Wide-band waveguide and ridge waveguide T-junctions for diplexer applications," *IEEE Trans. Microwave Theory Tech.*, Vol. 41, 2166–2173, Dec. 1993.

11. Pyle, J. R., "The cutoff wavelength of the TE_{10} mode in ridged rectangular waveguide of any aspect ratio," *IEEE Trans. Microwave Theory Tech.*, Vol. MTT-14, 175–183, Apr. 1966.
12. Craven, G. F. and C. K. Mok, "The design of evanescent mode waveguide bandpass filters for a prescribed insertion loss characteristics," *IEEE Trans. Microwave Theory Tech.*, Vol. MTT-19, 295–308, Mar. 1971.
13. Synder, R. V., "New application of evanescent mode waveguide to filter design," *IEEE Trans. Microwave Theory Tech.*, Vol. MTT-25, 1013–1021, Dec. 1977.